

RESEARCH

Open Access

LncRNA LINC00520 aggravates cell proliferation and migration in lung adenocarcinoma via a positive feedback loop



Wen Huang^{1†}, Xinxing Wang^{2†}, Fubing Wu^{2*} and Fanggui Xu^{2*}

Abstract

Background: Lung adenocarcinoma (LUAD) is the most common histological subtype of primary lung cancer. To identify the biomarker of diagnosis for LUAD is of great significance. Long non-coding RNAs (lncRNAs) were previously revealed to exert vital effects in numerous cancers. LncRNA long intergenic non-protein coding RNA 520 (LINC00520) served as an oncogene in various cancers. Therefore, our study was specially designed to probe the role of LINC00520 in LUAD.

Results: LINC00520 expression was detected by RT-qPCR. Next, function of LINC00520 in LUAD was verified by in vitro loss-of-function experiments. DNA pull down, ChIP, RISC and luciferase reporter assays were conducted to reveal the regulatory mechanism of LINC00520. We found that LINC00520 was upregulated in LUAD. Additionally, LINC00520 upregulation is associated with the poor prognosis for patients with LUAD. Furthermore, LINC00520 downregulation suppressed LUAD cell proliferation and migration and induced cell apoptosis. Forkhead box P3 (FOXP3) is identified as the transcription factor to transcriptionally activate LINC00520. Moreover, LINC00520 positively upregulated FOXP3 expression via sponging miR-3611 in LUAD cells. Subsequently, rescue experiments delineated that miR-3611 downregulation or FOXP3 overexpression reversed the effects of silenced LINC00520 on proliferative and migratory capabilities in LUAD cells.

Conclusion: This study innovatively indicated that lncRNA LINC00520 facilitated cell proliferative and migratory abilities in LUAD through interacting with miR-3611 and targeting FOXP3, which may provide a potential novel insight for treatment of LUAD.

Keywords: Lung adenocarcinoma, LINC00520, FOXP3, Transcription factor, miR-3611

Introduction

Lung cancer is a leading cause of cancer-related death worldwide [1, 2]. Approximately 85% of lung cancer cases are non-small-cell lung cancers, of which lung adenocarcinoma (LUAD) is the most common histologic subtype [3, 4], accounting for about 40% of all lung cancer cases

[2]. Although most early-stage LUAD can be effectively treated by surgery, the prognoses of unresectable LUAD are poor with the 5-year survival rates less than 20% [5]. LUAD patients are usually diagnosed at advance stages with metastasis [6]. Thus, it is of great significance to find the biomarker affecting LUAD cell proliferation and migration.

With the development of next-generation sequencing, it has now been recognized that most complex eukaryotic genomes are noncoding RNAs (ncRNAs), including a family of transcripts with length of over 200 nucleotides termed long noncoding RNAs (lncRNAs) [7, 8].

*Correspondence: wfbwx@hotmail.com; xfg2007@sohu.com

[†]Wen Huang and Xinxing Wang have contributed equally to the work

² Department of Oncology, Sir Run Run Hospital of Nanjing Medical University, 109 Longmian Avenue, Jiangning District, Nanjing, China
Full list of author information is available at the end of the article



lncRNAs, functioning as miRNA sponges, have been characterized in cancer development and pathologies [9]. Many lncRNAs including ITGB1-DT [10], LINC01426 [11], UPLA1 [12] have been revealed to promote LUAD cell migration and invasion. Mechanistically, the competing endogenous RNA (ceRNA) pattern has been widely reported to be involved in LUAD progression [13–15]. The ceRNA network refers to that lncRNAs bind with microRNAs (miRNAs) to suppress the degradation of the targets of the miRNAs [16]. It has been previously reported that lncRNA long intergenic non-protein coding RNA 520 (LINC00520) served as the tumor promoter in melanoma [17], papillary thyroid carcinoma [18], and colorectal cancer [19] by serving as a ceRNA, while its role and regulatory mechanism in LUAD remain elusive.

Transcription factors (TFs) are considered to be the main regulators of gene expression [20–22]. TFs are ubiquitously expressed in many tissues and are implicated in many biological functions of embryogenesis, cellular proliferation, DNA replication, and differentiation [23]. TFs exert their dual functions: activator or repressor of gene expression [24, 25] by targeting promoter regions of their downstream molecules [26, 27]. We explored the potential TFs that can transcriptionally regulate LINC00520 in LUAD cells.

Our study focused on the biological role of LINC00520 in LUAD cells. In addition, the upstream TF and the downstream ceRNA pattern of LINC00520 were investigated. Our data implied that LINC00520 served as an oncogene in LUAD and might be used in future LUAD treatment.

Materials and methods

Tissue samples

Twenty pairs of LUAD specimens and adjacent non-tumor tissues were acquired from patients who did not receive any therapy before undergoing operation in Sir Run Run Hospital of Nanjing Medical University. Tissue specimens were obtained from patients who signed written informed consents. Research was performed in accordance with the Declaration of Helsinki and approval was obtained from the Ethics Committee of the Sir Run Run Hospital of Nanjing Medical University. Immediately after the operation, tissue samples were frozen in liquid nitrogen and maintained at -80°C .

Cell culture

LUAD cell lines (A549, H1975, H2030, H1435) and a normal human bronchial epithelial cell (BEAS-2B) were provided by the American Type Culture Collection (ATCC; Gaithersburg, MD, USA). Briefly, all cancer cells applied in this study were maintained in Dulbecco's modified

Eagle's medium (DMEM; Gibco, Waltham, MA, USA) containing 10% fetal bovine serum (FBS; Gibco, Waltham, MA, USA), 100 U/ml penicillin (Sigma-Aldrich, USA), and 100 mg/ml streptomycin (Sigma-Aldrich, USA) at 37°C with 5% CO_2 . BEAS-2B cell lines were cultured in Clonetics™ media.

Bioinformatics analysis

According to PROMO prediction version 3.0.2 (http://algen.lsi.upc.es/cgi-bin/promo_v3/promo/promoinit.cgi?dirDB=TF_8.3), 22 potential TFs (condition: within a dissimilarity margin less or equal than 0%) bound to promoters of LINC00520 were identified. Based on JASPAR database (<http://jaspar.genereg.net/>), potential binding sites of FOXP3 at the promoter region of LINC00520 (condition: threshold value greater than 90) were predicted, and the DNA motif of FOXP3 was exhibited. Survival analysis of LUAD patients with high or low expression of LINC00520 was predicted from Kaplan–Meier plotter (<https://kmplot.com/analysis/index.php?p=service>). Overlapped miRNAs binding with LINC00520 and FOXP3 were predicted by online tool DIANA lncBase Predicted v.2 (http://carolina.imis.athena-innovation.gr/diana_tools/web/index.php?r=lncbasev2/index-predicted) and miRDB (<http://mirdb.org/>).

Plasmids

The overexpression vector pcDNA™3.1/Hygro⁽⁺⁾ (catalogue number: V87020) was purchased from Invitrogen (Carlsbad, CA, USA). The construction of pcDNA3.1/LINC00520 or pcDNA3.1/FOXP3 was provided by GenePharma (Shanghai, China). The negative control shRNA vector (pGPU6/Neo; catalogue number: E-03) and shRNAs targeting LINC00520 or FOXP3 for silencing of LINC00520 or FOXP3 were purchased from GenePharma. The basic pmirGLO Dual-Luciferase miRNA Target Expression Vector (catalogue number: E1330) was provided by Promega. Construction of the pmirGLO plasmids containing the wild type (WT) or mutated (MUT) 3' untranslated region (3'UTR) of FOXP3 was provided by GenePharma and was used for evaluating binding between miR-3611 and FOXP3 3'UTR. The basic pGL3 Luciferase Reporter Vector (catalogue number: E1751) was purchased from Promega. Construction of the pGL3 plasmid containing the WT or MUT promoter of LINC00520 was provided by GenePharma and was used for evaluating binding between FOXP3 and LINC00520 promoter. The pRL Renilla Luciferase Control Reporter Vector (catalogue number: E2231; Promega) provides normalization for the pmirGLO and pGL3 plasmids.

Cell transfection

MiR-3611 mimics (inhibitor) and NC mimics (inhibitor) were supplied by GenePharma. A549 and H1975 cells were transfected with miR-3611 mimics (inhibitor) or NC mimics (inhibitor), empty pcDNA3.1, pcDNA3.1/LINC00520 or pcDNA3.1/FOXP3, shRNA, sh-LINC00520#1/2 or sh-FOXP3#1/2 by Lipofectamine 2000 (Invitrogen, Carlsbad, CA, USA). A549 and H1975 cells were transfected for 48 h. Additionally, RT-qPCR was applied to testify transfection efficiency.

Reverse transcription quantitative polymerase chain reaction (RT-qPCR)

Total RNA was extracted from frozen tissue samples or cultured cells using TRIzol reagent (Thermo Fisher Scientific) and was reverse transcribed into complementary DNA (cDNA) using a Reverse Transcription Kit (Invitrogen). RT-qPCR analysis was conducted with a SYBR Green Premix PCR Master Mix (Roche, Mannheim, Germany) by an ABI HT9600 (Applied Biosystems, Foster City, CA, USA). Glyceraldehyde-3-phosphate dehydrogenase (GAPDH) was taken as the internal reference for LINC00520 and FOXP3. RNU6 (U6) was taken as the internal reference for miR-3611. The $2^{-\Delta\Delta CT}$ method was utilized to calculate the relative quantification. Relative primer sequences are listed as follows:

- LINC00520, forward: 5'-AGGAACAGCATCAGAGTC-3';
- reverse: 5'-TCTGACTCCTCCAGCT-3'.
- FOXP3, forward: 5'-AGGACTTCCTCAAGCACTG-3';
- reverse: 5'-CTCCAGAGCTCTACCATCTC-3'.
- YY1, forward: 5'-GAATCTGCTAGGGCTGCAC-3';
- reverse: 5'-CACCTTCTGCACAGACGTG-3'.
- XBPI, forward: 5'-CGATTCTGGCGGTATTGA-3';
- reverse: 5'-AAAGGGAGGCTGGTAAGG-3'.
- GAPDH, forward: 5'-TCATTCCTGGTATGACATCC-3';
- reverse: 5'-GTCTTACTCCTTGAGGCC-3'.
- miR-3611, forward: 5'-GTGAAGAAAGAAATCTTAGCGGC-3';
- reverse: 5'-CTCTACAGCTATATTGCCAGCCAC-3'.
- miR-6512-3p, forward: 5'-TTCCAGCCCTTCTAATGGTAGG-3';
- reverse: 5'-CTCTACAGCTATATTGCCAGCCAC-3'.
- miR-6720-5p, forward: 5'-ATTGTGGCGCACCGAGTT-3';
- reverse: 5'-GCCTACCAGGGCTGGAAGAA-3'.
- U6, forward: 5'-ATACAGAGAAAGTTAGCACGG-3';
- reverse: 5'-GGAATGCTTCAAAGAGTTGTG-3'.

CCK-8 assay

After transfection, cell viability was measured by a Cell Counting Kit-8 (CCK-8; Dojindo, Kyushu, Japan) under the manufacturer's guidance. A549 or H1975 cells (1×10^3) were plated into 96-well plates for 0, 1, 2, 3, and 4 days. CCK-8 solution was added into plates to cultivate cells for 2 h at 37 °C. Optical density at wavelength of 450 nm was measured by a microplate reader (Thermo Fisher Scientific).

Colony formation assay

A549 or H1975 cells (1×10^3) were plated into 6-well plates at 37 °C with 5% CO₂. After 2 weeks, colonies were fixed by 4% paraformaldehyde (Solarbio, Beijing, China) for 10 min, and dyed by crystal violet (Beyotime, Nantong, China) for 5 min when colonies were visible. The plates were photographed, and the number of colonies was manually counted.

Flow cytometry analysis

Transfected cells were collected and resuspended with phosphate buffered saline (PBS). After being cultured at 6-well plates for 48 h, A549 or H1975 cells were fixed in 70% ethanol pre-cooled with ice for 2 h. Quantification of apoptosis was measured by flow cytometry (Thermo Fisher Scientific) after staining with Annexin V-FITC/PI (BD Biosciences, San Jose, CA, USA).

Wound healing assay

After transfection, A549 or H1975 cells seeded in 6-well plates were subjected to serum starvation for 4 h. Thereafter, the wound was stimulated by straight scratching in the cell monolayer using a sterile 200- μ L pipette tip. After gently scraping the scratched monolayer cells twice with serum-free medium, the wound was healed in complete medium for 24 h. Then, after the wound was formed, photographs of the wound width at 0 h and 24 h were captured using an inverted microscope, respectively.

Western bolt

Cells were lysed with lysis buffer containing protease inhibitors (50 mM Tris-HCl pH 8; 50 mM NaCl; 0.5% NP-40). Total protein was extracted from tissues and cells using radioimmunoprecipitation assay buffer (Thermo Fisher Scientific, Inc.). Protein concentration was determined using a bicinchoninic acid assay. The extracted total protein (20 μ g) was subjected to 10% sodium dodecyl sulfate-polyacrylamide gel electrophoresis (SDS-PAGE; Solarbio, Beijing, China) and transferred to polyvinylidene fluoride (PVDF) membranes (Sigma-Aldrich, Shanghai, China). After PVDF membranes was blocked with 5% skim milk at 25 °C for 1 h, the primary antibodies were added for incubation overnight. Primary

antibodies included anti-BAX (1/1000; ab32503; Abcam), anti-Bcl-2 (1/1000; ab32124; Abcam), anti-E-cadherin (1/10000; ab40772; Abcam), anti-N-cadherin (1/5000; ab76011; Abcam) and anti-GAPDH (1/2500; ab9485; Abcam). After adding secondary antibodies, proteins were visualized by an enhanced chemiluminescence detection kit (Amersham Pharmacia Biotech, UK) and analyzed by a Bio-Rad image analysis system (Bio-Rad, CA, USA). Unprocessed original scans of the western blots were provided in Additional file 1.

DNA pull down assay

A DNA pull-down test kit (Gzscbio, Guangzhou, China) was utilized under manufacturer's guidance to analyze the interactions between proteins and DNA for identifying the transcription factors for LINC00520. The DNA pull down assay was conducted according to a previous study [28]. In brief, cells were lysed followed by centrifugation at 12,000 rpm at 4 °C for 15 min. Probe targeting LINC00520 promoter was designed and labeled with desthiobiotin, and then bound with streptavidin-containing magnetic beads, followed by cultivation with cellular protein extracts at 4 °C overnight, and separation by SDS-PAGE. The eluates were subjected to western blotting analysis for detection of potential transcription factors.

Chromatin immunoprecipitation (ChIP) assay

A chromatin immunoprecipitation (ChIP) assay was performed using a Magna ChIP (Millipore, Billerica, MA) under manufacturer's instruction. In brief, DNA fragments were sonicated in LUAD cells and collected by centrifugation, which were then immunoprecipitated with anti-FOXP3 (1/30, ab15206, Abcam) and negative control anti-IgG (1/30, ab172730, Abcam). Subsequently, DNA fragment binding with the above antibodies was purified by DNA-purifying slurry and detected by PCR using primers targeting the promoter sequences of LINC00520.

Luciferase reporter assay

The pmirGLO plasmids containing WT FOXP3 3'UTR were co-transfected with NC mimics, or miR-3611 mimics, or miR-3611 mimics + pcDNA3.1/LINC00520 into A549 or H1975 cells with Lipofectamine 2000 (Invitrogen). Similarly, the pmirGLO plasmids containing MUT FOXP3 3'UTR were co-transfected with NC mimics, or miR-3611 mimics, or miR-3611 mimics + pcDNA3.1/LINC00520 into A549 or H1975 cells. The pGL3 plasmids containing WT or MUT promoter sequences of LINC00520 were co-transfected with pcDNA3.1, or pcDNA3.1/FOXP3 into A549 or H1975 cells using Lipofectamine 2000. Dual-Luciferase Reporter Assay System (Promega) was utilized to confirm luciferase

activities. Relative firefly luciferase activity was normalized to *renilla* luciferase activity.

Subcellular fractionation

The cytoplasmic and nuclear extracts were extracted from A549 or H1975 cells by Nuclear and Cytoplasmic Extraction Reagents (Thermo Fisher Scientific). RNAs isolated from nucleus or cytoplasm were performed RT-qPCR analysis. The levels of U6 (nucleus control), GAPDH (cytoplasm control), and LINC00520 were determined by PCR, respectively.

RNA immunoprecipitation (RIP) assay

RNA immunoprecipitation (RIP) experiment was conducted using Magna RIP™ RNA-Binding Protein Immunoprecipitation Kit (Millipore, Billerica, MA) under manufacturer's instructions. A549 and H1975 cells were lysed in complete RIPA lysis buffer, and the cell extract was incubated with magnetic beads conjugated with anti-Ago2 or control anti-IgG for 6 h at 4 °C. The beads were washed and then incubated with Proteinase K to detach proteins. RT-qPCR was utilized to detect relative expression of co-precipitated RNAs.

Statistical analysis

Data were analyzed by SPSS (SPSS Inc., Chicago, IL, USA). Results were denoted as means ± standard deviation. Kaplan Meier and Log-rank test were performed for survival curve. Comparison between two groups was evaluated by Student's t test. Comparison among three groups was assessed with analysis of variance (ANOVA) followed by Turkey's *post-hoc* test. Each experiment was repeated three times in triplicate. $p < 0.05$ was considered as statistically significant.

Results

LINC00520 was upregulated in LUAD and facilitated cell proliferation and migration in LUAD

Under RT-qPCR result, LINC00520 presented upregulation in LUAD tissues than in adjacent non-tumor tissues (Fig. 1a). In addition, LINC00520 expression was higher in LUAD cells (A549, H1975, H2030, H1435) than normal cell line (BEAS-2B) (Fig. 1b). In addition, Kaplan Meier analysis revealed that LINC00520 upregulation implied unfavorable prognosis of patients with LUAD (Fig. 1c). Subsequently, we knocked down LINC00520 expression in A549 and H1975 cells by transfection with sh-LINC00520 plasmids with sh-NC as scramble control. LINC00520 expression under sh-LINC00520 transfection was downregulated in LUAD cells compared with that in scramble control group (Fig. 1d). LINC00520 silencing repressed cell viability and reduced number of colonies, indicating that LINC00520 silencing impeded

(See figure on next page.)

Fig. 1 LINC00520 presented upregulation in LUAD and promoted proliferation and migration in LUAD cells. **a** LINC00520 level in LUAD tissues and adjacent non-tumor ones was examined through RT-qPCR. **b** RT-qPCR testified LINC00520 expression in 4 LUAD cells and BEAS-2B cell line. **c** Kaplan Meier analysis depicted the survival curve for prognosis of patients with LUAD. **d** RT-qPCR detected knockdown efficacy of sh-LINC00520#1/2 in LUAD cells. **e** CCK-8 assay was adopted to confirm viability of LUAD cells under LINC00520 silencing. **f** Colony formation assay assessed LUAD cell proliferation affected by LINC00520 knockdown. **g, h** Apoptosis rate of LUAD cells influenced by LINC00520 downregulation was analyzed by flow cytometric analysis. **i** Western blotting was conducted to reveal the effects of sh-LINC00520 on Bax and Bcl-2 protein levels in A549 and H1975 cells. **j** Migrative ability of LUAD cells was detected by wound healing experiment after LINC00520 downregulation. **k** Western blot analysis examined protein expression levels of EMT markers affected by LINC00520 silencing. ** $p < 0.01$, *** $p < 0.001$

LUAD cell proliferation (Figs. 1e, f). Number of colonies in A549 and H1975 cells transfected with sh-LINC00520#1 (or sh-LINC00520#2) is 47% (or 53%) of the sh-NC group. Furthermore, LINC00520 knockdown facilitated the apoptosis of LUAD cells, as evidenced by the flow cytometry analysis and western blotting (Fig. 1g–i). Moreover, the migratory ability of LUAD cells was suppressed by LINC00520 depletion (Fig. 1j). The EMT process in LUAD was determined via measuring EMT marker protein levels using western blot. We found that E-cadherin level showed significant increase, and N-cadherin level showed significant decrease under LINC00520 depletion (Fig. 1k).

FOXP3 transcriptionally induced upregulation of LINC00520 in LUAD cells

Based on PROMO prediction, 22 potential TFs were predicted to bind to promoters of LINC00520 (Fig. 2a). To probe interaction between TFs and LINC00520 promoter, DNA pull down assay was conducted. Results revealed that three TFs (FOXP3, YY1 and XBP-1) showed enrichment in LINC00520 promoter sense group than in antisense group (Fig. 2b). As presented in Fig. 2c, FOXP3 was upregulated in LUAD cells, and the other two TFs were not. Additionally, FOXP3 expression illustrated the upregulation in LUAD tissues compared to that in adjacent non-tumor tissues (Fig. 2d). Therefore, FOXP3 was proved to be the transcriptional activator of LINC00520 in LUAD. Subsequently, we successfully overexpressed (or silenced) FOXP3 expression by transfection with pcDNA3.1+/FOXP3 (or sh-FOXP3#1/2) (Fig. 2e). FOXP3 overexpression upregulated LINC00520 expression and FOXP3 silencing downregulated LINC00520 expression in LUAD cells (Fig. 2f). Five potential binding sites of FOXP3 at the promoter region of LINC00520 were predicted (Fig. 2g). ChIP experiment revealed that DNA sequence containing site 5 showed an enrichment in FOXP3 immunoprecipitation product (Fig. 2h), which suggested abundant binding of FOXP3 with LINC00520 promoter at site 5. Additionally, it was found from luciferase reporter assay that FOXP3 overexpression induced increase in luciferase activity of pGL3 vector containing WT LINC00520 promoter (Fig. 2i).

LINC00520 interacted with miR-3611 to regulate FOXP3

Subsequently, we investigated the regulatory mechanism of LINC00520 on FOXP3. LINC00520 knockdown suppressed FOXP3 expression and LINC00520 upregulation increased FOXP3 expression (Fig. 3a, b), which suggested that LINC00520 positively modulated FOXP3 expression. Next, results of subcellular fractionation experiment revealed the cytoplasmic localization of LINC00520 in A549 and H1975 cells (Fig. 3c), indicating the post-transcriptional regulation of LINC00520 on downstream genes. As shown by the Venn pattern in Fig. 3a, there were three putative miRNAs binding with both LINC00520 and FOXP3. Moreover, expression of the three miRNAs in 4 LUAD cells and BEAS-2B cell line was testified by RT-qPCR. As a result, only miR-3611 was downregulated in LUAD cells (Fig. 3e). Additionally, it was demonstrated from RT-qPCR result that miR-3611 expression presented downregulation in LUAD tissues compared to that in adjacent non-tumor tissues (Fig. 3f). We overexpressed miR-3611 using miR-3611 mimics and NC mimics was used as a negative control. It turned out that miR-3611 expression was increased by miR-3611 mimics transfection (Fig. 3g). Additionally, miR-3611 binding site on LINC00520 or FOXP3 was predicted with DIANA or miRDB, as shown in Fig. 3h. Luciferase reporter assay indicated that upregulation of LINC00520 increased luciferase activity of FOXP3-WT, which was suppressed under miR-3611 overexpression, and luciferase activity of FOXP3-Mut presented no significant alteration under the same condition (Fig. 3i). Results of RIP assay revealed that miR-3611 was co-immunoprecipitated with LINC00520 and FOXP3 by Ago2, which revealed that miR-3611 bound to LINC00520 and FOXP3 in RNA-induced silencing complex (RISC) (Fig. 3j).

LINC00520 functioned to be an oncogene in LUAD cells though positive feedback loop of LINC00520/miR-3611/FOXP3

To explore whether LINC00520 modulates cell proliferation and migration by the miR-3611/FOXP3 axis, we performed rescue experiments. First, it was verified that miR-3611 expression was silenced under transfection of miR-3611 inhibitor (Fig. 4a). Next, inhibitory effect

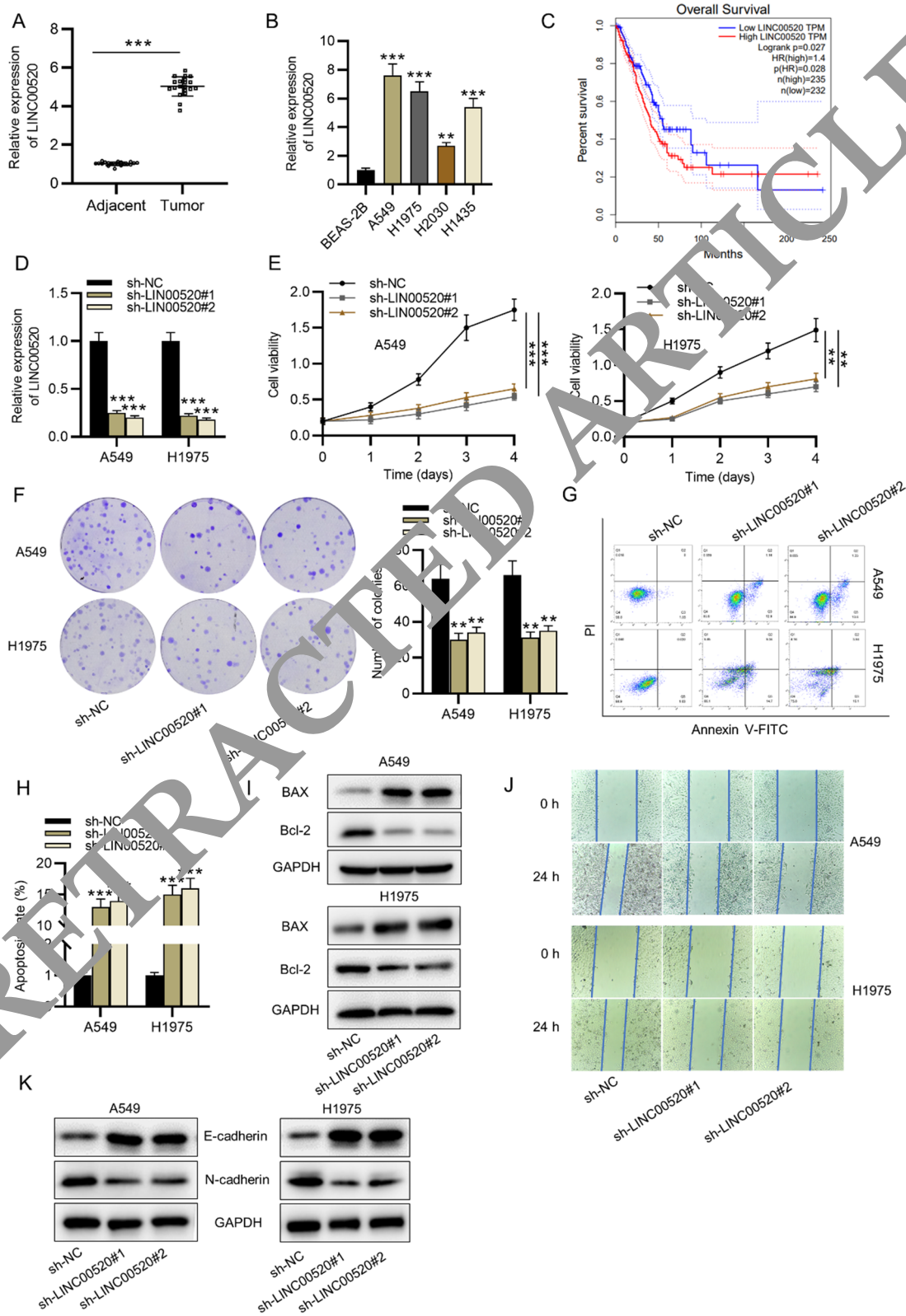


Fig. 1 (See legend on previous page.)

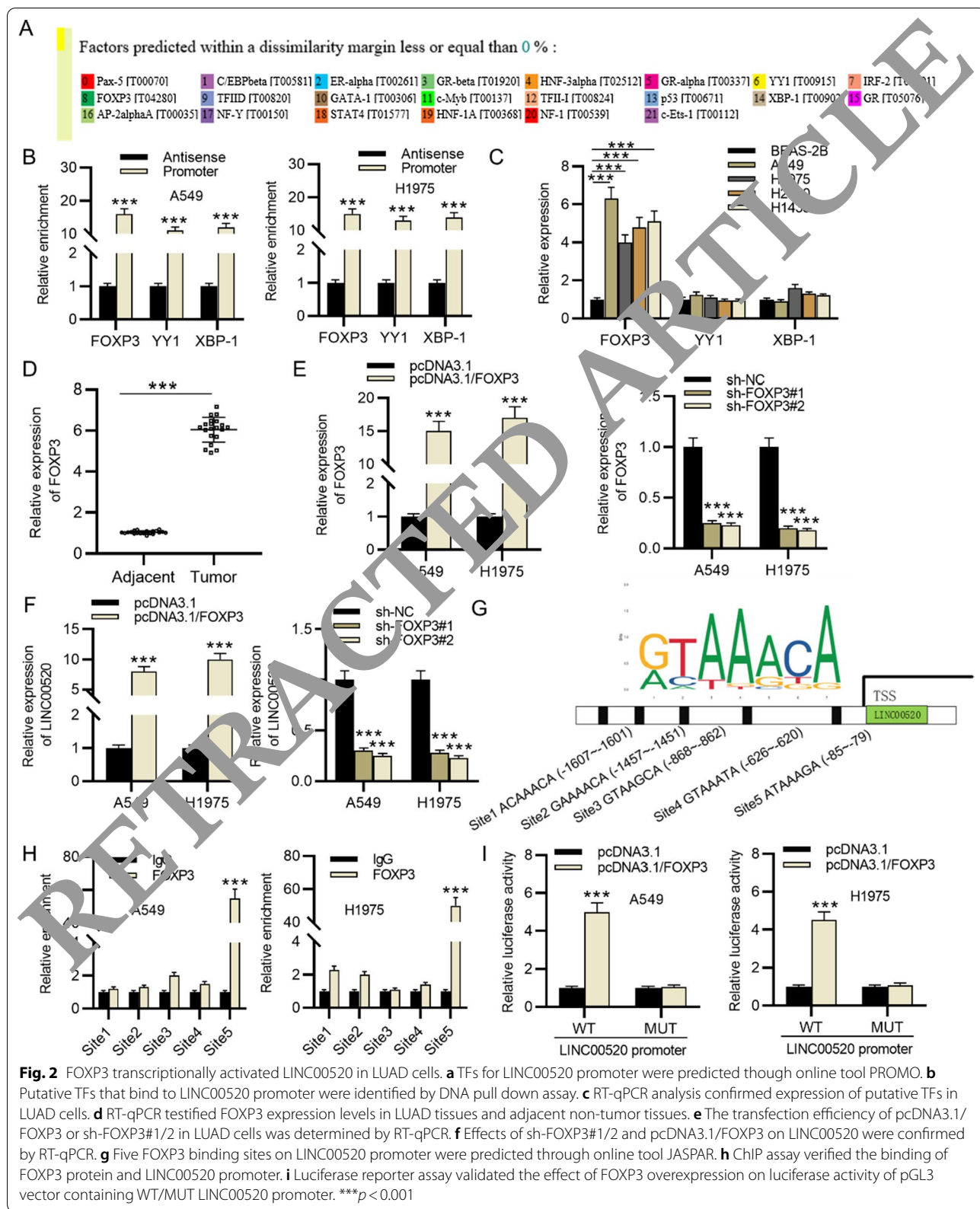


Fig. 2 FOXP3 transcriptionally activated LINC00520 in LUAD cells. **a** TFs for LINC00520 promoter were predicted through online tool PROMO. **b** Putative TFs that bind to LINC00520 promoter were identified by DNA pull down assay. **c** RT-qPCR analysis confirmed expression of putative TFs in LUAD cells. **d** RT-qPCR testified FOXP3 expression levels in LUAD tissues and adjacent non-tumor tissues. **e** The transfection efficiency of pcDNA3.1/FOXP3 or sh-FOXP3#1/2 in LUAD cells was determined by RT-qPCR. **f** Effects of sh-FOXP3#1/2 and pcDNA3.1/FOXP3 on LINC00520 were confirmed by RT-qPCR. **g** Five FOXP3 binding sites on LINC00520 promoter were predicted through online tool JASPAR. **h** ChIP assay verified the binding of FOXP3 protein and LINC00520 promoter. **i** Luciferase reporter assay validated the effect of FOXP3 overexpression on luciferase activity of pGL3 vector containing WT/MUT LINC00520 promoter. ****p* < 0.001

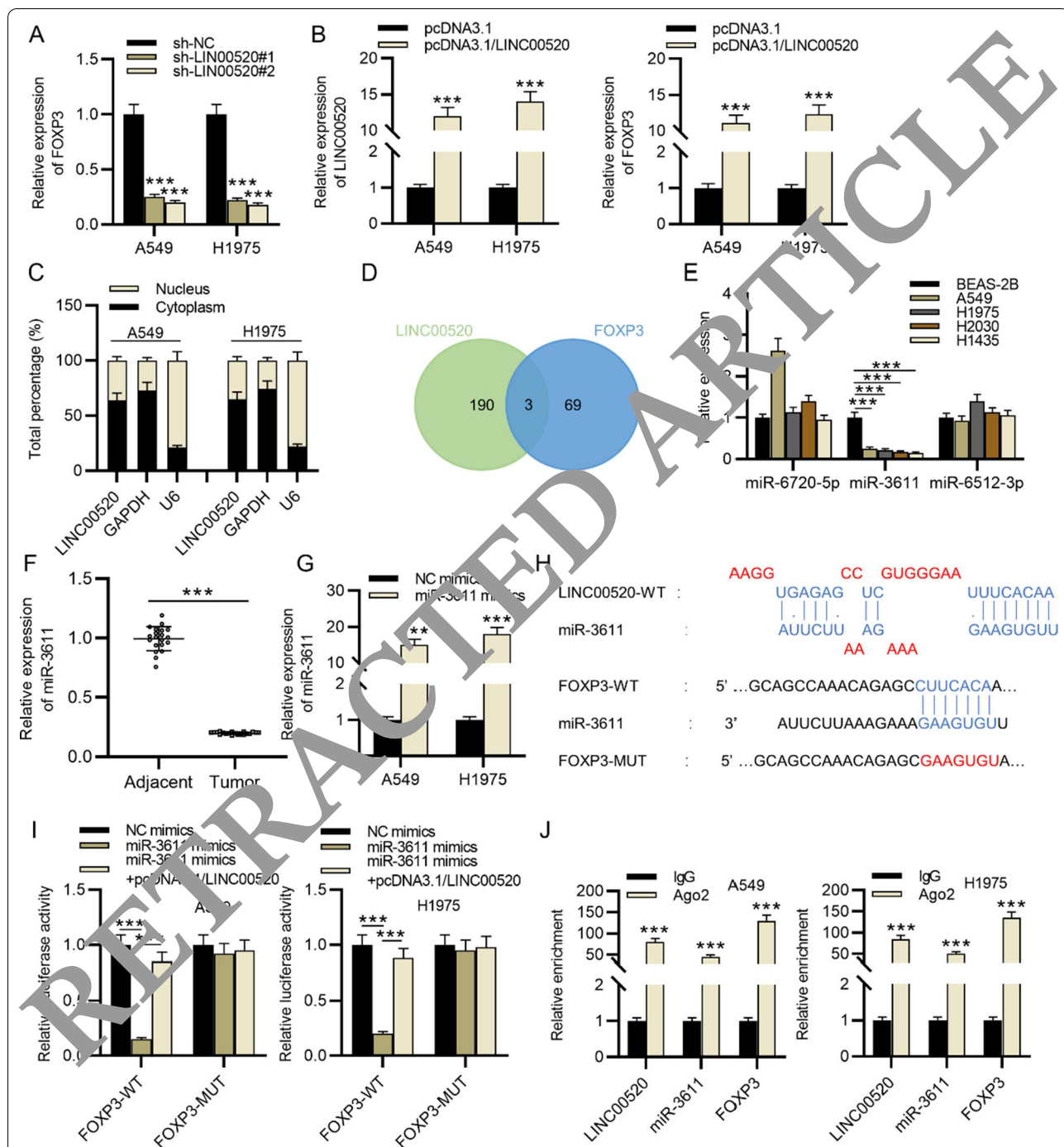


Fig. 3 LINC00520 upregulated FOXP3 expression by binding to miR-3611. **a** Effect of sh-LINC00520#1/2 on FOXP3 expression was testified by RT-qPCR. **b** The overexpression efficiency of LINC00520 and the impact of LINC00520 upregulation on FOXP3 expression in LUAD cells were determined by RT-qPCR. **c** Subcellular localization of LINC00520 was confirmed with subcellular fractionation assay in LUAD cells. **d** Venn pattern showed three putative shared miRNAs for LINC00520 and FOXP3 with online tool DIANA and miRDB. **e** RT-qPCR was conducted to detect expression of 3 putative miRNAs in LUAD cells. **f** MiR-3611 levels in LUAD tissues and adjacent non-tumor tissues was determined via RT-qPCR. **g** The overexpression efficiency of miR-3611 in LUAD cells was tested through RT-qPCR analysis. **h** Binding sequence between miR-3611 and LINC00520 (FOXP3) were predicted through DIANA and miRDB, respectively. **i** Luciferase reporter experiment verified binding ability of miR-3611 and FOXP3. **j** Enrichment of miR-3611, LINC00520, FOXP3 precipitated by Ago2 was further validated by RIP assay. ****p* < 0.001

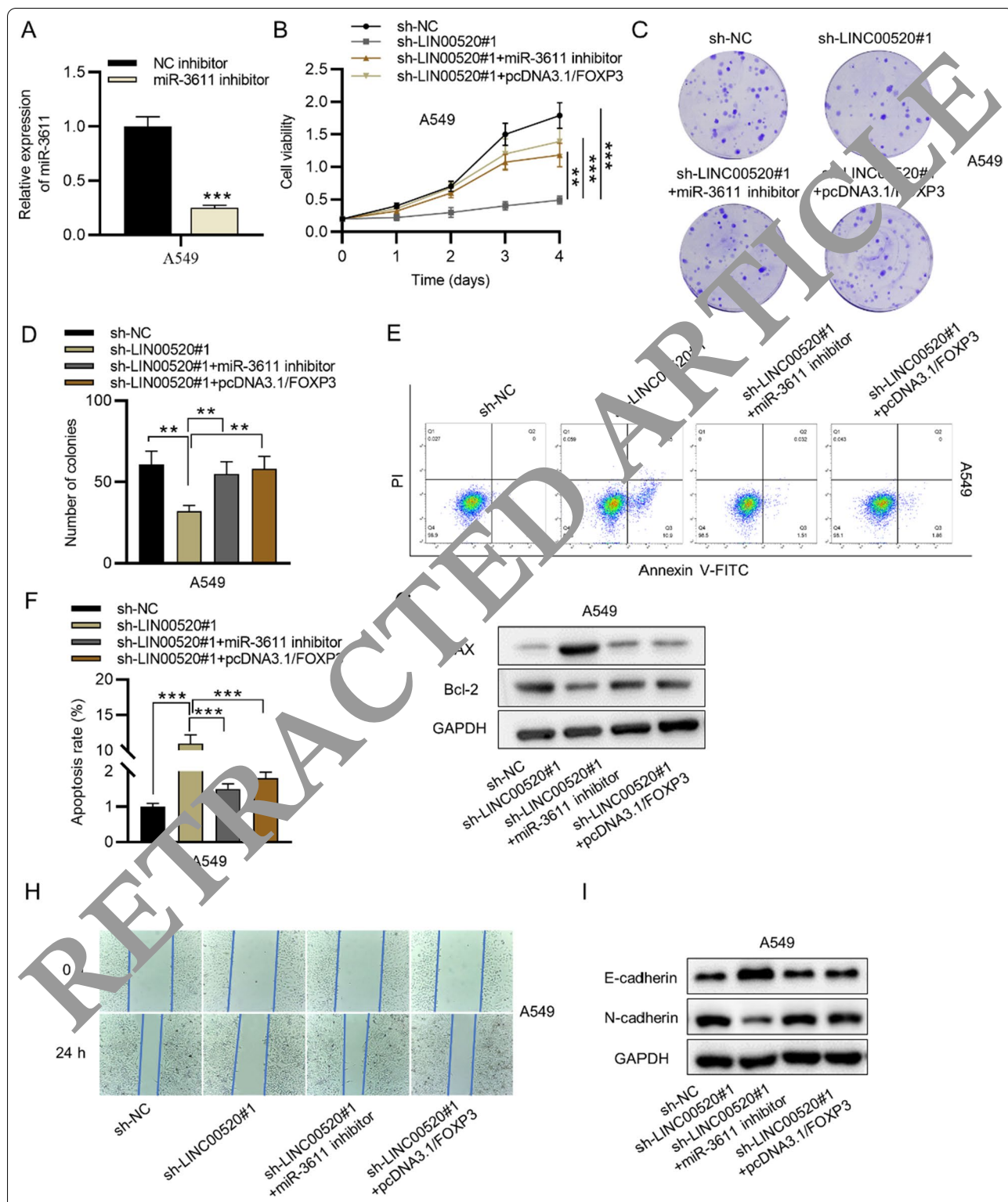


Fig. 4 LINC00520 facilitated proliferation and migration in LUAD cells through modulating the LINC00520/miR-3611/FOXP3 axis. **a** Silencing efficiency of miR-3611 in LUAD cells was measured through RT-qPCR. **b** Cell viability under indicated transfection was confirmed via CCK-8 assay. **c, d** Colony formation assay was performed to detect LUAD cell proliferative ability in indicated transfection groups. **e-g** LUAD cell apoptosis in each group was detected by flow cytometric analysis and western blotting. **h** Wound healing assay determined the migration of LUAD cells after indicated transfection. **i** Western blot measured protein expression of EMT markers in LUAD cells under co-transfection. ** $p < 0.01$, *** $p < 0.001$

of LINC00520 silencing on viability of A549 cells was partially rescued under miR-3611 downregulation or FOXP3 upregulation (Fig. 4b). Additionally, pcDNA3.1/FOXP3 or miR-3611 inhibitor rescued the decreased number of colonies mediated by LINC00520 downregulation (Fig. 4c, d). Number of colonies in A549 cells transfected with sh-LIN00520#1 is 52% of the sh-NC group. Number of colonies in A549 cells cotransfected with sh-LIN00520#1 + miR-3611 inhibitor (or sh-LIN00520#1 + pcDNA3.1/FOXP3) is 172% (or 181%) of the sh-LIN00520#1 group. Furthermore, increased apoptosis of A549 cells caused by LINC00520 silencing was counteracted by miR-3611 downregulation or FOXP3 upregulation (Fig. 4e–g). Additionally, miR-3611 knockdown or FOXP3 overexpression rescued the suppressed migratory ability of LUAD cells caused by LINC00520 depletion (Fig. 4h). Moreover, the increase in E-cadherin and decrease in N-cadherin under LINC00520-knockdown was rescued by miR-3611 depletion or FOXP3 elevation (Fig. 4i).

Discussion

Recently, lncRNAs have been found to function as oncogenes in modulating cell proliferation and migration [29, 30]. As previously reported, LINC00520 has an oncogenic effect on melanoma [17], papillary thyroid carcinoma [18], and colorectal cancer [19]. We revealed that LINC00520 expression was upregulated in LUAD cells and tissues. Online Kaplan Meier analysis showed that higher LINC00520 expression implied poorer prognosis of LUAD patients. Functionally, silencing of LINC00520 inhibited proliferative and migratory abilities and promoted apoptosis of LUAD cells. These results revealed that LINC00520 functioned as an oncogene in LUAD. lncRNAs can be transcriptionally activated by their upstream TFs to exert regulatory effects in LUAD [31, 32]. FOXP3 is a forkhead lineage-transcription factor and presents upregulated expression in various cancers including breast cancer [33], colorectal cancer [34], tongue squamous cell carcinoma [35] and cervical cancer [36]. In addition, FOXP3 has been reported to promote cell proliferation, invasion and EMT in non-small cell lung cancer [37]. Expression level of FOXP3 was significantly positively correlated with somatic mutation burden in LUAD patients [38]. We identified that FOXP3 was a TF for LINC00520 to induce its upregulation and was overexpressed in LUAD tissues and cell lines.

Furthermore, we found that FOXP3 expression can be positively modulated by LINC00520 in LUAD cells. Results from subcellular fractionation assay suggested the cytoplasmic localization of LINC00520 in LUAD

cells, which implied that LINC00520 post-transcriptionally modulated FOXP3 expression. The ceRNA network is a typical regulatory pattern occurring in the cytoplasm of cancer cells [39, 40]. The present study identified that miR-3611 was downregulated in LUAD tissues and cell lines. The role of miR-3611 in cancers has not been revealed by other studies, while Cheng Liu et al. revealed that exosome derived miR-3611 is upregulated in subjects with increased low-density lipoprotein cholesterol serum levels [41], and Sigrun Lange et al. revealed that miR-3611 is similar between SARS-CoV-2 and the human genome [42]. Our findings indicated that miR-3611 can bind with both LINC00520 and FOXP3. MiR-3611 degraded FOXP3 by targeting its 3'UTR. Additionally, LINC00520 upregulated FOXP3 expression by functioning as a miR-3611 sponge. Finally, a series of rescue assays further suggested that LINC00520 contributed to LUAD cell proliferation and migration via sponging miR-3611 to upregulate FOXP3.

In conclusion, FOXP3-induced LINC00520 was an oncogene in LUAD and induced proliferation and migration as well as suppressed apoptosis in LUAD cells. Mechanistically, LINC00520 served as a ceRNA against miR-3611 to suppress the degradation of FOXP3 caused by miR-3611. Our study potentially provides a new vision for treatment of LUAD.

Supplementary Information

The online version contains supplementary material available at <https://doi.org/10.1186/s12890-021-01657-6>.

Additional file 1. Unprocessed original scans of the western blots.

Acknowledgements

Thank you for all lab members involved in this study.

Authors' contributions

WH and XW carried out the experiments. WH, FW, FX and XW analyzed the data. WH, XW, FW and FX drafted the manuscript. All authors agreed to be accountable for all aspects of the work. All authors have read and approved the final manuscript.

Funding

Not applicable.

Availability of data and materials

The datasets used and/or analysed during the current study available from the corresponding author on reasonable request.

Declarations

Ethics approval and consent to participate

Research was performed in accordance with the Declaration of Helsinki and approval was obtained from the Ethics Committee of the Sir Run Run Hospital of Nanjing Medical University. Tissue specimens were obtained from patients who signed informed consent.

Consent for publication

Not applicable.

Competing interests

The authors declare that there exists no conflict of interest.

Author details

¹Department of Oncology, The Fourth Affiliated Hospital of Nanjing Medical University, Nanjing 210000, Jiangsu, China. ²Department of Oncology, Sir Run Run Hospital of Nanjing Medical University, 109 Longmian Avenue, Jiangning District, Nanjing, China.

Received: 9 February 2021 Accepted: 31 August 2021

Published online: 08 September 2021

References

- Cheung CHY, Juan HF. Quantitative proteomics in lung cancer. *J Biomed Sci.* 2017;24(1):37.
- Bodor JN, Kasireddy V, Borghaei H. First-line therapies for metastatic lung adenocarcinoma without a driver mutation. *J Oncol Pract.* 2018;14(9):529–35.
- Hutchinson BD, Shroff GS, Truong MT, Ko JP. Spectrum of lung adenocarcinoma. *Semin Ultrasound CT MR.* 2019;40(3):255–64.
- Balzer BWR, Loo C, Lewis CR, Trahair TN, Anazodo AC. Adenocarcinoma of the lung in childhood and adolescence: a systematic review. *J Thorac Oncol.* 2018;13(12):1832–41.
- Devarakonda S, Govindan R, Morgensztern D. Mastering the complex targeted therapy for non-small cell lung cancer. *Cancer Cell.* 2020;38(3):320–2.
- Gridelli C, Rossi A, Carbone DP, Guarize J, Karachaliou N, Morici F, et al. Non-small-cell lung cancer. *Nat Rev Dis Primers.* 2015;1:1500.
- Charles Richard JL, Eichhorn PJA. Platforms for Investigating LncRNA Functions. *SLAS Technol.* 2018;23(6):493–506.
- Paraskevopoulou MD, Hatzigeorgiou AG. Analyzing miRNA-lncRNA Interactions. *Methods Mol Biol (Clifton, NJ).* 2016;1302:271–86.
- Jarroux J, Morillon A, Pinskaya M. Historical discovery, and classification of lncRNAs. *Adv Exp Med Biol.* 2017;1008:1–46.
- Chang R, Xiao X, Fu Y, Zhang C, Zhu X, Gao Y, ITGB1-ITGB4-DT facilitates lung adenocarcinoma progression via forming a positive feedback loop with ITGB1/Wnt/ β -catenin/MYC. *Front Cell Dev Biol.* 2021;9:631259.
- Liu X, Yin Z, Xu L, Liu H, Jiang L, Gu S, et al. Upregulation of LINC01426 promotes the progression and suppresses in lung adenocarcinoma by enhancing the level of SHH protein to activate the hedgehog pathway. *Cell Death Dis.* 2021;12(2):173.
- Han X, Jiang H, Qi J, Li J, Yang J, Tian Y, et al. Novel lncRNA UPLA1 mediates tumorigenesis and prognosis in lung adenocarcinoma. *Cell Death Dis.* 2020;11(10):999.
- Huang H, Lu H, Zhang J, Xu L, Xu S, et al. Exploring the effect of differentially expressed long non-coding RNAs driven by copy number variation by competing endogenous RNA network by mining lung adenocarcinoma data. *Front Cell Dev Biol.* 2020;8:627436.
- Li H, Ma Q, Zhang G, Shen Z, Zhang Y, Bai J, et al. Linc00426 accelerates lung adenocarcinoma progression by regulating miR-455-5p as a molecular sponge. *Cell Death Dis.* 2020;11(12):1051.
- Jia Y, Duan Y, Liu T, Wang X, Lv W, Wang M, et al. LncRNA TTN-AS1 promotes migration, invasion, and epithelial mesenchymal transition of lung adenocarcinoma via sponging miR-142-5p to regulate CDK5. *Cell Death Dis.* 2019;10(8):573.
- Thomson DW, Dinger ME. Endogenous microRNA sponges: evidence and controversy. *Nat Rev Genet.* 2016;17(5):272–83.
- Luan W, Ding Y, Yuan H, Ma S, Ruan H, Wang J, et al. Long non-coding RNA LINC00520 promotes the proliferation and metastasis of malignant melanoma by inducing the miR-125b-5p/EIF5A2 axis. *J Exp Clin Cancer Res CR.* 2020;39(1):96.
- Sun Y, Shi T, Ma Y, Qin H, Li K. Long noncoding RNA LINC00520 accelerates progression of papillary thyroid carcinoma by serving as a competing endogenous RNA of microRNA-577 to increase Sphk2 expression. *Cell cycle (Georgetown, Tex).* 2020;19(7):787–800.
- Jin XH, Hong YG, Li P, Hao LQ, Chen M. Long noncoding RNA LINC00520 accelerates the progression of colorectal cancer by serving as a competing endogenous RNA of microRNA-577 to increase HSP27 expression. *Hum Cell.* 2020;33:683–94.
- Khazaei N, Rastegar-Pouyani S, O'Toole N, Wee P, Mohammadniaei A, Yaqubi M. Regulating the transcriptomes that mediate the conversion of fibroblasts to various nervous system neural cell types. *J Cell Physiol.* 2018;233(4):3603–14.
- Perez-Rueda E, Hernandez-Guerrero R, Martinez-Nunez MA, Armenta-Medina D, Sanchez I, Ibarra JA. Abundance, diversity, and domain architecture variability in prokaryotic DNA-binding transcription factors. *PLoS ONE.* 2018;13(4):e0195332.
- Mahdevar G, Sadeghi M, Nezhari-Dalini Z. Transcription factor binding sites detection by using alignment-based approach. *J Theor Biol.* 2012;304:96–102.
- Ustiyev V, Bolteev I, Zhang Y, Han L, Xu Y, Yutzey KE, et al. FOXF1 transcription factor promotes lung morphogenesis by inducing cellular proliferation in fetal lung mesenchyme. *Dev Biol.* 2018;443(1):50–63.
- Kim JG, Huddgett MB. Tomato bHLH132 transcription factor controls growth and defense and is activated by *Xanthomonas euvesicatoria* effector XopD during pathogenesis. *Mol Plant-microbe Interact MPMI.* 2019;32(12):1614–22.
- Harayan S, Bryant G, Shah S, Berrozpe G, Ptashne M. OCT4 and SOX2 work as transcriptional activators in reprogramming human fibroblasts. *Cell Rep.* 2017;20(7):1585–96.
- Yu CP, Li WH. Predicting transcription factor binding sites and their cognate transcription factors using gene expression data. *Methods Mol Biol (Clifton, NJ).* 2017;1629:271–82.
- Crocker J, Noon EP, Stern DL. The soft touch: low-affinity transcription factor binding sites in development and evolution. *Curr Top Dev Biol.* 2016;117:455–69.
- Singh B, Nath SK. Identification of proteins interacting with single nucleotide polymorphisms (SNPs) by DNA pull-down assay. *Methods Mol Biol (Clifton, NJ).* 2019;1855:355–62.
- Sanchez Calle A, Kawamura Y, Yamamoto Y, Takeshita F, Ochiya T. Emerging roles of long non-coding RNA in cancer. *Cancer Sci.* 2018;109(7):2093–100.
- Ulitsky I, Bartel DP. lincRNAs: genomics, evolution, and mechanisms. *Cell.* 2013;154(1):26–46.
- Ren P, Hong X, Chang L, Xing L, Zhang H. USF1-induced overexpression of long noncoding RNA WDFY3-AS2 promotes lung adenocarcinoma progression via targeting miR-491-5p/ZNF703 axis. *Mol Carcinog.* 2020;59(8):875–85.
- Cui Y, Zhang C, Ma S, Guan F. TFAP2A-induced SLC2A1-AS1 promotes cancer cell proliferation. *Biol Chem.* 2021;402:717–27.
- Zhang G, Zhang W, Li B, Stringer-Reasar E, Chu C, Sun L, et al. MicroRNA-200c and microRNA-141 are regulated by a FOXP3-KAT2B axis and associated with tumor metastasis in breast cancer. *Breast Cancer Res BCR.* 2017;19(1):73.
- Sun X, Feng Z, Wang Y, Qu Y, Gai Y. Expression of Foxp3 and its prognostic significance in colorectal cancer. *Int J Immunopathol Pharmacol.* 2017;30(2):201–6.
- Li K, Huang SH, Lao XM, Yang L, Liao GQ, Liang YJ. Interaction of cancer cell-derived Foxp3 and tumor microenvironment in human tongue squamous cell carcinoma. *Exp Cell Res.* 2018;370(2):643–52.
- Luo Q, Zhang S, Wei H, Pang X, Zhang H. Roles of Foxp3 in the occurrence and development of cervical cancer. *Int J Clin Exp Pathol.* 2015;8(8):871–30.
- Yang S, Liu Y, Li MY, Ng CSH, Yang SL, Wang S, et al. FOXP3 promotes tumor growth and metastasis by activating Wnt/ β -catenin signaling pathway and EMT in non-small cell lung cancer. *Mol Cancer.* 2017;16(1):124.
- Kadara H, Choi M, Zhang J, Parra ER, Rodriguez-Canales J, Gaffney SG, et al. Whole-exome sequencing and immune profiling of early-stage lung adenocarcinoma with fully annotated clinical follow-up. *Ann Oncol.* 2017;28(1):75–82.

39. Karreth FA, Pandolfi PP. ceRNA cross-talk in cancer: when ce-bling rivalries go awry. *Cancer Discov.* 2013;3(10):1113–21.
40. Smillie CL, Sirey T, Ponting CP. Complexities of post-transcriptional regulation and the modeling of ceRNA crosstalk. *Crit Rev Biochem Mol Biol.* 2018;53(3):231–45.
41. Liu C, Lai Y, Ying S, Zhan J, Shen Y. Plasma exosome-derived microRNAs expression profiling and bioinformatics analysis under cross-talk between increased low-density lipoprotein cholesterol level and ATP-sensitive potassium channels variant rs1799858. *J Transl Med.* 2020;18(1):459.
42. Lange S, Arisan ED, Grant GH, Uysal-Onganer P. MicroRNAs for virus pathogenicity and host responses, identified in SARS-CoV-2 genomes, may play roles in viral-host co-evolution in putative zoonotic host species. *Viruses.* 2021;13(1):117.

Publisher's Note

Springer Nature remains neutral with regard to jurisdictional claims in published maps and institutional affiliations.

RETRACTED ARTICLE

Ready to submit your research? Choose BMC and benefit from:

- fast, convenient online submission
- thorough peer review by experienced researchers in your field
- rapid publication on acceptance
- support for research data, including large and complex data types
- gold Open Access which fosters wider collaboration and increased citations
- maximum visibility for your research: over 100M website views per year

At BMC, research is always in progress.

Learn more biomedcentral.com/submissions

